

## FINITE ELEMENT SIMULATION OF CHAOTIC VIBRATIONS OF A BEAM WITH NON-LINEAR BOUNDARY CONDITIONS

R. I. K. MOORTHY,† A. KAKODKAR,‡ H. R. SRIRANGARAJAN§ and S. SURYANARAYAN¶

†Reactor Engineering Division, ‡Reactor Design and Development Group,  
Bhabha Atomic Research Centre, Bombay-400 085, India

§Department of Mechanical Engineering, ¶Department of Aeronautical Engineering,  
Indian Institute of Technology, Bombay-400 076, India

(Received 14 July 1992)

**Abstract**—The solution of the chaotic vibration of non-linear mechanical systems involves the numerical integration of the governing equations of motion over a large time duration. This time duration should be adequately large to ensure that the transients die down and the solution captures the steady-state chaos. This demands that the integration scheme be stable, and accurate. The scheme which has found wide acceptance for chaotic problems is the fourth-order Runge–Kutta method.

However, the Runge–Kutta method is not a preferred integration scheme for engineering solutions because it calls for four equation solutions per time-step and a small time-step to get accurate results from ‘stiff equations’ produced by the engineering structures. These drawbacks have restricted the study of chaos to single-or-limited number of degrees of freedom.

This paper is an attempt to solve the chaotic vibration problem of structures with non-linear boundary conditions by the finite element method. The solution is attempted for the cantilever beam with one side-stop for which experimental results are available in the literature. This particular class of non-linearity has been chosen because of its abundance in and significance to the real-life structures.

The authors’ study shows that the temporally discrete solution of the spatially discrete model could capture the phenomenon of chaos. The authors expect this study to be useful for identifying the chaotic regimes for these structures in the physical coordinates of forcing amplitude and frequency. This, in turn, could be used for a more accurate prediction of fretting wear-limited life of these components.

### 1. INTRODUCTION

There are many mechanical systems which allow some play between the assembled components. Although the small clearances may not always be a design requirement, it is not possible to eliminate them totally due to the manufacturing tolerances. There are also systems where a predefined gap or clearance is provided by design. The gap between heat exchanger tubes and the baffle plates, between pipe-lines and snubbers, between components and the displacement arrestors, etc., are all examples of systems with designed clearances. These clearances produce a non-linear boundary condition which could lead to chaotic response as demonstrated by Moon and Shaw [1] for a simple cantilever.

There have been many attempts to simulate by the finite element method, the dynamic behaviour of such systems with gaps [2–10]. However, most of them attempt to extract information regarding maximum contact force which could be used to predict the fretting wear-limited life of the system. It appears that the analysis to study the characteristics of the long duration response themselves have not been pursued much, which in many cases could be chaotic.

Even though many engineering systems with non-linear boundary conditions could cause chaotic response, the study of chaotic vibrations has been

highly restricted. The present-day techniques seem to attempt solution of highly simplified single degree of freedom or very limited number of degrees of freedom models through integration schemes like the fourth-order Runge–Kutta method. There has been no attempt to study such systems through popular numerical techniques used by engineers for dynamic simulation of structures. The motivation for this study has been the identification by Moon [11] of tests to confirm whether these can also give solutions where the response is known to be chaotic.

This paper is an attempt to simulate the interaction of the cantilever beam with one-side stop, studied by Moon and Shaw [1], by the finite element method.

### 2. FINITE ELEMENT MODEL

The equations of equilibrium for a system assembled by a set of finite elements could be written as [12–15]

$$[K]\{y\}_{t+\Delta t} + [C]\{\dot{y}\}_{t+\Delta t} + [M]\{\ddot{y}\}_{t+\Delta t} = \{P\}_{t+\Delta t} \quad (1)$$

where  $[K]$  is the stiffness matrix of the assembly,  $[C]$  is the damping matrix,  $[M]$  is the mass matrix,  $\{P\}$  is the external load vector at time  $t + \Delta t$ , and  $\{y\}_{t+\Delta t}$ ,  $\{\dot{y}\}_{t+\Delta t}$ ,  $\{\ddot{y}\}_{t+\Delta t}$  are the displacement, velocity and acceleration vectors at time  $t + \Delta t$ .

### 2.1. Stiffness matrix [k]

The formation of a stiffness matrix for a straight, uniform beam element has been discussed in detail by many authors [12–15]. For the beam studied by Moon and Shaw [1], no effect of transverse shear deformation or axial load need be considered.

### 2.2. Mass matrix [M]

In the finite element formulation of the mass matrix, there are two approaches [12, 13, 15, 16]—the lumped mass and the consistent mass. The most common approach is the ‘lumped mass’ wherein the inertia forces are considered as part of the body forces.

An excellent review of the advantages and disadvantages with respect to accuracy and computational effort of the two methods of defining the mass matrix is available in [13].

The applicability of the two approaches for the particular problem of a beam with non-linear support conditions has been studied by Shin *et al.* [4] in connection with the vibro-impact response of a heat exchanger tube with baffle plates. They have concluded that lumped mass approach is appropriate for this class of problems.

For the present problem under study, the translational and rotational inertias have been lumped at each degree of freedom.

### 2.3. Damping matrix [C]

The various numerical treatments to account for damping have been reviewed in [23]. For the present computation, the damping matrix is formed based on the Rayleigh proportional damping where the damping matrix is a linear combination of mass and stiffness matrices

$$C = \beta[M] + \gamma[K]. \quad (2)$$

The constants  $\beta$  and  $\gamma$  are determined from two known values of frequency and modal damping ratio. For the solution of the problem reported here, a value of  $\beta = 0$  and  $\gamma = 3.146 \times 10^{-4}$  has been used. This corresponds to a modal damping constant ( $2\omega\zeta$ ) of 0.017 for the first mode obtained in the experiment reported in [1].

## 3. SIMULATION OF NON-LINEAR BOUNDARY CONDITIONS

Restraints with gaps are simulated by an element of non-linear stiffness  $K_{NL}$ . The non-linear element can be described in terms of piece-wise linear force–deflection curve as shown in Fig. 1. The energy loss in impact is represented by a local damper of value  $C_{NL}$ . Such a scheme of representation has given acceptable results as reported by Sauvé and Teper [8] and Hibbit and Karlsson [6].

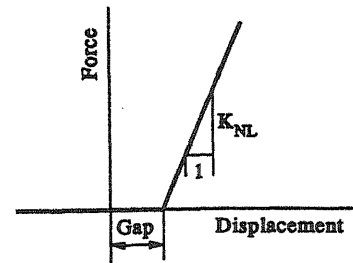


Fig. 1. Simulation of gap.

However, Fricker [24] suggested the following force–deflection relationship.

$$F = k(Ur - g)^{3/2}, \quad \text{if } Ur > g$$

$$F = 0, \quad \text{if } Ur \leq g, \quad (3)$$

where  $F$  is the contact force,  $k$  is the stiffness,  $Ur$  is the relative displacement between the two contacting surfaces, and  $g$  is the gap.

For the present problem of cantilever both the above representations have been studied. It is seen that the linear representation gives a Poincaré plot closer to the experimental Poincaré plot obtained by Moon and Shaw [1].

The equation of motion (1) can now be written separating the linear and non-linear contributions and including the Rayleigh damping as

$$M\ddot{y}_{i+\Delta t} + \beta M\dot{y}_{i+\Delta t} + \gamma K\dot{y}_{i+\Delta t} + C_{NL}\dot{y}_{i+\Delta t} + Ky_{i+\Delta t} + K_{NL}y_{i+\Delta t} = P_{i+\Delta t}.$$

In the present problem, the non-linearities  $K_{NL}$  and  $C_{NL}$  are confined to just one node. To avoid the reformation of the stiffness matrix and its solution, the non-linear contributions can be transformed into an equivalent non-linear load. Thus, eqn (1) becomes

$$M\ddot{y}_{i+\Delta t} + \beta M\dot{y}_{i+\Delta t} + \gamma K\dot{y}_{i+\Delta t} + Ky_{i+\Delta t} = P_{i+\Delta t} - F_{NL}, \quad (4)$$

where

$$F_{NL} = K_{NL}y_{i+\Delta t} + C_{NL}\dot{y}_{i+\Delta t}.$$

## 4. SOLUTION SCHEME

To obtain the solution of the governing equations of motion, a numerical integration technique is used. The step-by-step integration method can be applied either to the coupled equations of motion as in eqn (4) or the uncoupled equations of motion after modal decomposition by the mode superposition method.

For linear systems with few and well-defined modes contributing to the total response, the modal superposition method could give reasonably accurate results. The method has the advantage of greatly reduced computing effort. The modal superposition method has been used by many to solve non-linear

boundary condition problems as well [24, 27]. However, as Fricker [24] concludes further work is required to validate the method for impacting oscillators under harmonic loading. Applicability of mode super-position method for chaotic vibration problem is being studied separately. However, since the direct integration of the coupled equations of motion includes the response in all the frequencies, it is considered appropriate for the problem of chaotic vibrations.

Of the direct step-by-step integration procedures, the fourth-order Runge-Kutta method seems to be the preferred algorithm for chaos in lower order systems. It has an error of the order of  $(\Delta t)^5$ , but requires four equation solutions per time-step. The finite element model of structures produces stiff equations, i.e. they characterize structures whose highest natural frequency is very much greater than the lowest ( $\omega_{\max} \gg \omega_{\min}$ ). Even for solving linear problems by Runge-Kutta method, such stiff equations need very small time-steps and so the method is not very popular for FEM applications. For non-linear chaotic problems, modelled by FEM, the time-step would be too very small to undertake any long duration solution.

Belytschko [22] has discussed the advantages and disadvantages and the stability and accuracy of the commonly used numerical algorithms in FEM. Belytschko also gives guidelines for choosing the appropriate integration method. The problem of the beam with a side-stop clearly falls into the category of 'inertial' problem and so implicit time integration is the appropriate one for the solution.

A number of implicit integration schemes are in common use in FEM and they have been reviewed by many [12, 13, 22, 26]. It has been found by many [9, 12, 22, 25, 26] that Newmark method [28] with operator constants of  $\delta = 0.5$  and  $\alpha = 0.25$ , which is unconditionally stable, is appropriate for this class of problem. This scheme has also been assessed for its applicability to this class of chaotic problems by the authors through solution of SDOF models.

#### 4.1. The integration scheme

The integration scheme is as summarized below. The method is based on the assumption

$$\dot{y}_{t+\Delta t} = \dot{y}_t + [(1-\delta)\ddot{y}_t + \delta\ddot{y}_{t+\Delta t}]\Delta t \quad (5)$$

$$y_{t+\Delta t} = y_t + \dot{y}_t \cdot \Delta t + [(1/2 - \alpha)\ddot{y}_t + \alpha\ddot{y}_{t+\Delta t}]\Delta t^2, \quad (6)$$

where  $\alpha$  and  $\delta$  are parameters to be chosen by the analyst. These parameters determine the accuracy and stability of the scheme. For unconditional stability

$$\delta \geq 0.5 \quad \text{and} \quad \alpha \geq (2\delta + 1)^2/16.$$

Artificial positive damping is introduced if  $\delta > 0.5$  and negative damping if  $\delta < 0.5$ . If  $\delta = 0.5$  and  $\alpha = 0$ ,

Newmark's method reduces to the central difference method which is an explicit method and found useful for wave propagation problem. If  $\delta = 0.5$  and  $\alpha = 1/6$ , the scheme becomes the linear acceleration scheme which is only conditionally stable. If  $\delta = 0.5$  and  $\alpha = 0.25$ , the method is proven to be unconditionally stable. The method is, then, called the constant average-acceleration method or the trapezoidal method. It is also seen that with these values of  $\delta$  and  $\alpha$ , there are no amplitude errors introduced for linear problems.

The present problem of the cantilever represented by eqn (4) when operated on by eqns (5) and (6) could be shown to be [8]

$$\bar{K}y_{t+\Delta t} = \bar{P}_{t+\Delta t} - F_{NL}, \quad (7)$$

where

$$\bar{K} = K \left[ 1 + \frac{\gamma\delta}{\alpha\Delta t} \right] + M \left[ \frac{1 + \beta\delta\Delta t}{\alpha\Delta t^2} \right]$$

and

$$\begin{aligned} \bar{P}_{t+\Delta t} = & P_{t+\Delta t} + M \left[ \left\{ \frac{1}{\alpha\Delta t^2} + \frac{\delta\beta}{\alpha\Delta t} \right\} y_t \right. \\ & + \left\{ \frac{1}{\alpha\Delta t} - \beta \left( 1 - \frac{\delta}{\alpha} \right) \right\} \dot{y}_t \\ & + \left. \left\{ \left( \frac{1}{2} - \alpha \right) - \frac{\beta\Delta t}{2} \left( 2 - \frac{\delta}{\alpha} \right) \right\} \ddot{y}_t \right] \\ & + K \left[ \frac{\gamma\delta}{\alpha\Delta t} y_t + \left( \frac{\delta}{\alpha} - 1 \right) \dot{y}_t \right. \\ & + \left. \frac{\gamma\Delta t}{2} \left( \frac{\delta}{\alpha} - 2 \right) \ddot{y}_t \right] \end{aligned}$$

$$\begin{aligned} F_{NL,t+\Delta t} = & K_{NL}y_{t+\Delta t} + \frac{\delta}{\alpha\Delta t} C_{NL}\dot{y}_{t+\Delta t} \\ & - C_{NL} \left[ \frac{\delta}{\alpha\Delta t} \dot{y}_t + \left( \frac{\delta}{\alpha} - 1 \right) \ddot{y}_t \right. \\ & + \left. \frac{\Delta t}{2} \left( \frac{\delta}{\alpha} - 2 \right) \ddot{\ddot{y}}_t \right]. \end{aligned}$$

The solution at time  $t + \Delta t$  is iterative in nature because non-linear stiffness and damping forces are dependent on displacement. The initial trial value of  $F_{NL}$  for the iteration is obtained by linear extrapolation of  $F_{NL}$  at  $t$  and  $t - \Delta t$ .

The convergence of the iteration is measured by the ratio of the difference between the current and the previous iterates for  $F_{NL}$  and the current value of  $F_{NL}$ . The convergence of the order  $1.0 \times 10^{-6}$  is normally achieved within a few iterations. If not, the time-step is reduced which hastens the convergence. A mathematical treatment of such a convergence criterion is dealt with in [8].

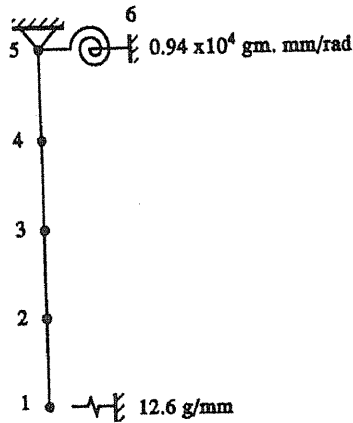


Fig. 2. FEM model of cantilever beam with one-side stop.

#### 4.2. Time-step error control

In addition to the control on step length to ensure convergence of  $F_{NL}$ , the errors associated with time stepping solution need to be contained. Ma and Bathe [10] and Belytschko and Shoerberle [25] have used an energy balance criteria to check and improve the accuracy of the solution. However, both the methods apply the error correction on the displacements keeping the time-step constant. However, Hibbit and Karlsson [6] and Sauvé and Teper [8] used a variable time-stepping algorithm based on the error in the equation of motion at half-time step. The concept is as follows.

By solving the dynamic equilibrium equation at discrete steps, it has been ensured that the system is in equilibrium at these times, namely,  $t$ ,  $t + \Delta t$ ,  $t + 2\Delta t$ , etc. The Newmark method (trapezoidal rule) allows one to obtain the displacement, velocity and acceleration at any intermediate point assuming a linear variation of the acceleration between two solution points. For any point  $t + \lambda\Delta t$ , they can be derived as

$$\ddot{y}_{t+\lambda\Delta t} = \frac{(y_{t+\Delta t} - y_t)}{\alpha\Delta t^2} \cdot \lambda - \frac{\dot{y}_t \cdot \lambda}{\alpha\Delta t} + \ddot{y}_t \left(1 - \frac{\alpha\lambda}{2}\right)$$

$$y_{t+\lambda\Delta t} = y_t + (y_{t+\Delta t} - y_t)\lambda^3 + \dot{y}_t(1 - \lambda^2)\lambda\Delta t + \ddot{y}_t(1 - \lambda)\lambda^2 \frac{\Delta t^2}{2}$$

$$\dot{y}_{t+\lambda\Delta t} = \frac{(y_{t+\Delta t} - y_t)}{\alpha\Delta t} \delta\lambda^2 + \dot{y}_t \left(1 - \frac{\delta}{\alpha}\lambda^2\right) + \ddot{y}_t \left(1 - \frac{\delta\lambda}{2\alpha}\right)\lambda\Delta t.$$

These could be used to calculate a 'residual' at any time within the time-step.

$$\text{RES} = Ky_{t+\lambda\Delta t} + M\ddot{y}_{t+\lambda\Delta t} + C\dot{y}_{t+\lambda\Delta t} - P_{t+\lambda\Delta t} + F_{NL_{t+\lambda\Delta t}}.$$

Based on numerical experiments, it has been reported [6, 8] that this residual increases at a fast rate when the error associated with the time-stepping solution becomes significant. Karlsson and Hibbit [6] have found that if the half-step residual is of the order of  $1.0 \times 10^{-2}P$ , the time-stepping solution has excellent accuracy. Sauvé and Teper [8] have used a tolerance on the residual based on the maximum forces that occur in the solution. They also caution about too small a tolerance on the residual as they feel that the tolerance may be related to the terms higher than second order in the Taylor series expansion for displacement and acceleration. So, too small a tolerance could result in no satisfaction of the criterion of algorithm even though the solution could have good accuracy.

The effect of this tolerance has been studied by the authors for impacting SDOF oscillators. It is found that specifying the tolerance based on the forces at the particular step gives excellent results. A tolerance based on the maximum forces that occur in the solution, as suggested in [8] is too coarse. Accordingly, the solutions have been carried out with a tolerance specified as

$$\text{max. of } 1\% \text{ of } [(P - F_{NL}) \text{ spring force, damping force, inertia force}]$$

for each translational and rotational DOF.

#### 5. FEM MODEL OF THE CANTILEVER BEAM WITH ONE-SIDE STOP [1]

For a uniform cantilever of the geometry considered in [1], the theoretical natural frequencies are 5.34, 33.38 and 93.6 Hz. However, Moon and Shaw [1] have measured the natural frequencies as 4.3, 26 and 73 Hz. Such reduction from theoretical natural frequencies is very common in engineering structures. This is due to the small rotations that are rendered possible at the clamped end by the assembly methods adopted. This could be modelled analytically by incorporating a rotational spring of appropriate stiffness at the support location [18–20]. To

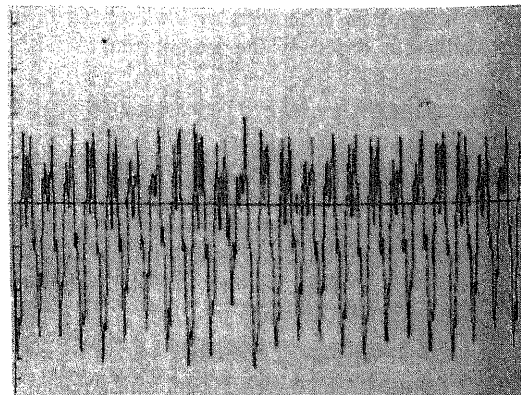


Fig. 3. Time history of strain for forcing frequency of 10.5 Hz and forcing amplitude of 3.7 mm peak-to-peak.

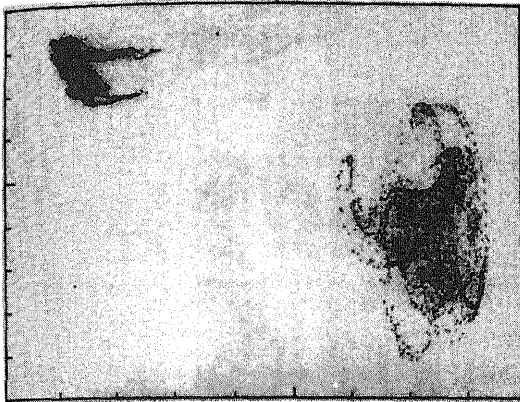


Fig. 4. Poincaré map of fixed end strain of the cantilever with one-side stop [1]. Forcing frequency = 10.5 Hz. Forcing amplitude = 3.7 mm peak-to-peak.

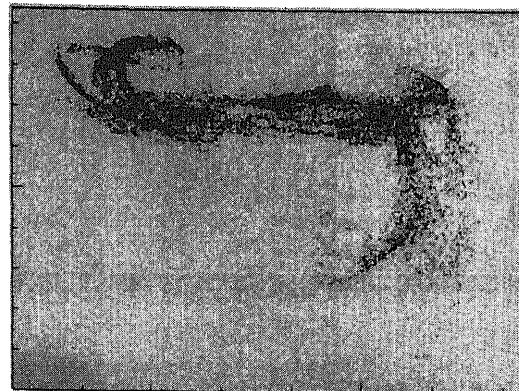


Fig. 6. Poincaré map of fixed end strain of the cantilever with one-side stop [1]. Forcing frequency = 10.2 Hz. Forcing amplitude = 4.0 mm peak-to-peak.

determine the appropriate value of rotational spring stiffness, the cantilever was modelled as shown in Fig. 2 and solved for eigenvalues using SAP-IV [21]. A spring stiffness of 0.93 kg cm/rad for the boundary element realizes nearly the same natural frequencies as obtained experimentally in [1].

#### 5.1. The stiffness of side stop

The goal of the side stop had been to provide a hinge support thereby obtaining a bilinear system [1]. The stiffness of the spring simulating the side stop has been derived by use of a boundary element of SAP-IV [20] at the free end of the cantilever. Twice the lowest stiffness of the boundary element for which the natural frequency goes up by a factor of 4.375 (i.e.  $f_n = 18.8$  Hz corresponding to a clamped-pinned case) has been used for the analysis. The actual stiffness of the stop could have been higher. The higher stiffness could result in the dominance of contribution from higher modes. However, Moon and Shaw [1] have filtered out the higher frequency in the results reported. It was, therefore, felt that use of a stiffness value higher than this may not be necessary for the present study. The actual value of stiffness

would however be important if the impact load and fretting wear estimates are to be made.

## 6. RESULTS

The results of the analysis for the four-element model shown in Fig. 2 are presented through the following figures. Figure 3 shows the time history of strain for excitation at 10.5 Hz and excitation amplitude of 3.7 mm peak-to-peak. Figure 4 shows the Poincaré map for excitation at 10.5 Hz and 3.7 mm peak-to-peak. Figure 5 shows the Poincaré map for excitation at 10.2 Hz and 4 mm peak-to-peak. Figure 6 shows the Poincaré map for excitation at 9.8 Hz and 4 mm peak-to-peak. Figure 7 shows the Poincaré plot for excitation at 10.5 Hz and amplitude of 3.7 mm peak-to-peak when the number of elements was increased to 15. With a large number of elements, the time-step becomes too small. To get over the problem the half-step tolerance has been increased to 10%. However, it is noted that the frequency range of chaos shifts slightly as the number of DOF and errors are increased to these values. This could also partly be due to deviation in the FEM model such as the mass of shim steel used for damping which has not been included in the model.

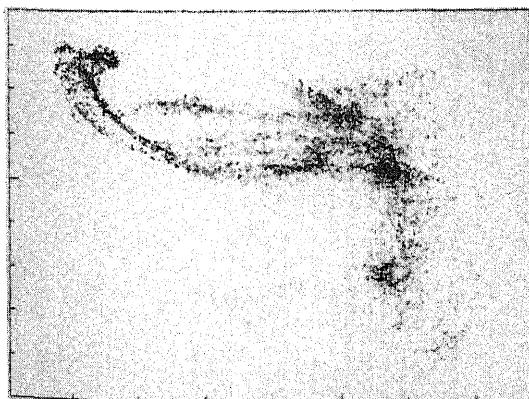


Fig. 5. Poincaré map of fixed end strain of the cantilever with one-side stop [1]. Forcing frequency = 9.8 Hz. Forcing amplitude = 4.00 mm peak-to-peak.

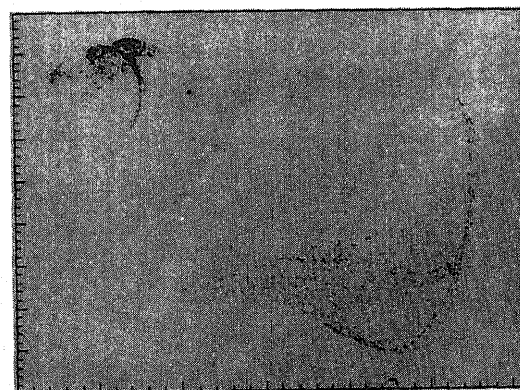


Fig. 7. Poincaré map at Fig. 3 with 15 element simulation.

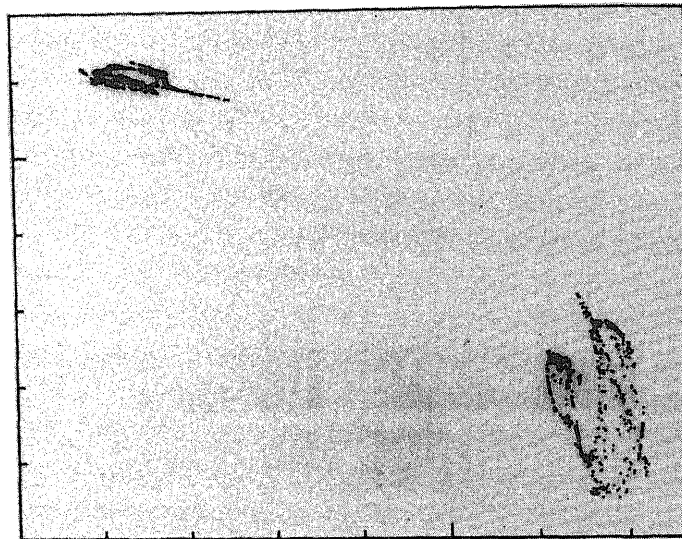


Fig. 8. Poincaré map of Fig. 4 for a three-element model.

Figures 8 and 9 shows the Poincaré plots when the number of elements was reduced to three. Figure 8 corresponds to an excitation of 3.7 mm peak-to-peak at 10.5 Hz and Fig. 9 to an excitation of 4.0 mm peak-to-peak at 9.8 Hz. These were solved with a half-step tolerance of 1%.

#### 7. DISCUSSION

Figures 10–12 show the experimental Poincaré plots presented in [1]. It can be observed on a comparison that the analytical results agree well with them. However, there are slight deviations like the scatter of the Poincaré points when the beam top is near the stops. This may be because the aluminium stops used in the experiment provides a large localized damping. Even though the formulation used here

could incorporate the non-linear damping  $C_{NL}$ , it was found that for significant  $C_{NL}$  values, the half-step error criterion is not easily satisfied. Still, the solution reported here is good enough for engineering applications where the chaotic regimes are to be identified. In addition, since the response of the structure is chaotic, such scatter is not expected to affect any engineering conclusions derived from these response data.

It is also observed that the spatial discretization, even if coarse, captures the chaotic response, as seen from the solution of a three-element model. It may, however, be cautioned that the comparison is based on experimental results where the signals were low pass filtered around 40 Hz. Since higher modes can contribute significantly to stress, the spatial discretization has to be finer if the signals are unfiltered or filtered at higher frequencies. For such a case, it is

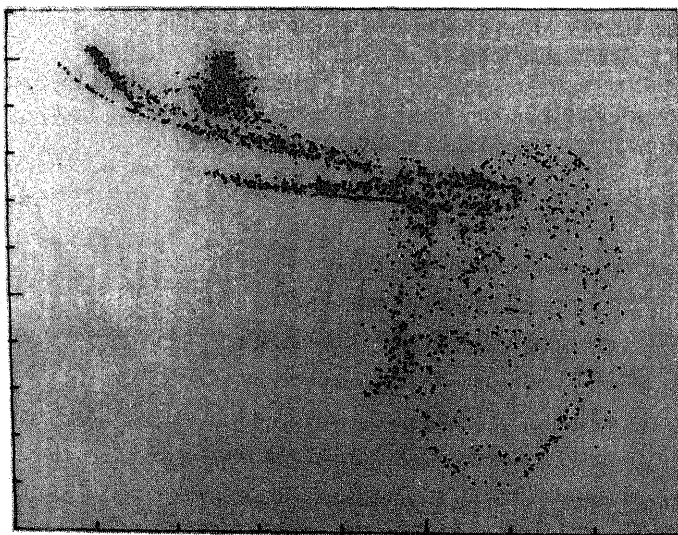


Fig. 9. Poincaré map of Fig. 5 for a three-element model.





Fig. 10. Experimental Poincaré map [1] corresponding to Fig. 4.

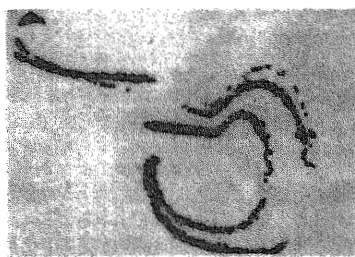


Fig. 11. Experimental Poincaré map [1] corresponding to Fig. 5.

also necessary to incorporate the appropriate values of  $K_{NL}$  and  $C_{NL}$ .

During the solution of various models, it was always found that period four motion becomes chaotic with increase of excitation. No period six motion was observed as reported in [1]. The authors could not offer any explanation for this.

### 8. CONCLUSIONS

Based on above discussion, it could be concluded that finite element method is capable of solving the dynamic response problems which could be chaotic. In other words, a spatially discrete representation and a temporarily discrete solution is capable of capturing the phenomenon of chaos in continuous elastic systems. Adequate checks have to be incorporated in the solution to contain the errors within small limits. This paper reports one such tool to study chaotic problems of one particular class.

To the best of our knowledge the chaotic responses have been solved only for very simplified models.

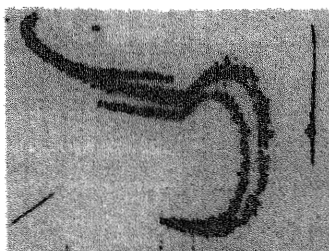


Fig. 12. Experimental Poincaré map [1] corresponding to Fig. 6.

Such models may not be useful to identify the regimes of chaos in the forcing-amplitude frequency planes. There are many engineering systems with design/manufacturing clearances, leading to non-linear support conditions and their chaotic regimes could be identified by a method of analysis similar to one reported here. Such analysis could become a significant input for a realistic prediction of the fretting wear limited life of the components, in case the response is chaotic.

### REFERENCES

1. F. C. Moon and S. W. Shaw, Chaotic vibrations of a beam with non-linear boundary conditions. *Int. J. Non-linear Mech.* **18**, 465-477 (1983).
2. R. J. Rogers and R. J. Pick, Factors associated with support plate forces due to heat exchanger tubes vibratory contact. *Nuclear Engng Des.* **44**, 247-253 (1977).
3. Y. S. Shin, D. E. Sass and J. A. Jendrzejczyk, Vibro-impact responses of a tube with tube-baffle interaction. ASME paper 78-PVP-20 (1978).
4. Y. S. Shin, D. E. Sass and J. A. Jendrzejczyk, Vibro-impact responses of a tube with tube-baffle interaction. ANL report ANL-CT-78-11 (1978).
5. K. J. Bathe and S. Gracewski, On non-linear dynamic analysis using sub-structuring and mode superposition. *Comput. Struct.* **13**, 699-707 (1981).
6. H. D. Hibbit and B. I. Karlsson, Analysis of pipe whip. EPRI report No. NO-1208 (1979).
7. R. G. Sauvé and W. W. Teper, Parametric studies of process equipment tube/support plate impact models. *Trans. of the 8th Conference on SMIRT, Belgium* (1985).
8. R. G. Sauvé and W. W. Teper, Impact simulation of process equipment tubes and support plate—a numerical algorithm. *ASME J. Pressure Vessel Technol.* **109**, 70-79 (1987).
9. E. C. Ting, S. S. Chen and M. W. Wambsgauss, Dynamics of component-support impact: an elastic analysis. *Nuclear Engng Des.* **52**, 235-244 (1979).
10. S. M. Ma and K. J. Bathe, On finite element analysis of pipe whip problems. *Nuclear Engng Des.* **37**, 413-430 (1976).
11. F. C. Moon, Non-linear dynamical systems. *Appl. Mech. Rev.* **38**, 1284-1286 (1985).
12. K. J. Bathe and E. L. Wilson, *Numerical Methods in Finite Element Analysis*. Prentice-Hall (1978).
13. R. D. Cook, *Concepts and Applications of Finite Element Analysis*. John Wiley (1981).
14. V. Ramamurthi, *Computer Aided Design in Mechanical Engineering*. Tata-McGraw-Hill, New Delhi (1987).
15. M. Paz, *Structural Dynamics—Theory and Computation*. Van Nostrand Reinhold (1985).
16. R. W. Clough and J. Penzien, *Dynamics of Structures*. McGraw-Hill (1987).
17. C. M. Harris, *Shock and Vibration Handbook*. McGraw-Hill (1987).
18. R. I. K. Moorthy, Report on early failure detection of 4-loop PWRs under the Indo-FRG bilateral agreement on peaceful uses of nuclear energy (1986).
19. V. Bauernfeind and R. I. K. Moorthy, Sensitivity studies using an analytical vibration model of a four-loop PWR. *19th Informal meeting on Reactor Noise*, Rome, 4-6 June (1986).
20. V. Bauernfeind, Vibration monitoring of a four-loop PWR: Model investigations of the sensitivity of the monitored signals on mechanical failures. *Progress in Nucl. Energy* **21**, 247-254 (1988).
21. K. J. Bathe, E. L. Wilson and F. E. Peterson, SAPIV—a structural analysis program for static and dynamic

- analysis of linear systems. Report EERC 73-11, College of Engineering, University of California, Berkeley, CA (1974).
22. T. Belytschko, A survey of numerical methods and computer programs for dynamic structural analysis. *Nuclear Engng Des.* **37**, 23–34 (1976).
  23. T. Belytschko and W. L. Mindle, The treatment of damping in transient computations. Presented at the winter annual meeting of the ASME on damping applications for vibration control. ASME publication No. AMD, Vol. 38 (1980).
  24. A. J. Fricker, The analysis of impacts in vibrating structures containing clearances between components. *Proceedings of International Conference on Numerical Methods for Transient and Coupled Problems, Venice, 9–13 July* (Edited by R. W. Lewis, E. Hinton and P. Bettess) (1984).
  25. T. Belytschko and D. F. Schoeberle, On unconditional stability of an implicit algorithm for non-linear structural dynamics. *ASME J. appl. Mech.* 865–869 (1975).
  26. T. J. R. Hughes and T. Belytschko, A precis of developments in computational methods for transient analysis. *ASME J. appl. Mech.* **50**, 1033–1041 (1983).
  27. B. J. Dobson, The Newmark and mode superposition methods for transient analysis of a linear structure—a case study. *Proceedings of the International Conference on Numerical Methods for Transient and Coupled Problems held in Venice, 9–13 July* (Edited by R. W. Lewis, E. Hinton and P. Bettess) (1984).
  28. N. Newmark, A method for computation for structural dynamics. *J. Engng Mech. Div., ASCE* **85**, No. EM3, 67–94 (1959).